Agricultural and Forest Meteorology 203 (2015) 118–130

Contents lists available at ScienceDirect

Agricultural and Forest Meteorology

journal homepage: www.elsevier.com/locate/agrformet

Experimental validation of a long-distance transport model for plant pathogens: Application to *Fusarium graminearum*

Aaron J. Prussin II[a,*], Linsey C. Marr[b], David G. Schmale III[a], Rob Stoll[c], Shane D. Ross[d]

[a] Department of Plant Pathology, Physiology, and Weed Science, Virginia Tech, Blacksburg, VA 24061-0390, United States
[b] Department of Civil and Environmental Engineering, Virginia Tech, Blacksburg, VA 24061-0246, United States
[c] Department of Mechanical Engineering, University of Utah, Salt Lake City, UT 84112, United States
[d] Department of Biomedical Engineering and Mechanics, Virginia Tech, Blacksburg, VA 24061-0219, United States

ARTICLE INFO

Article history:
Received 19 August 2014
Received in revised form
10 December 2014
Accepted 21 December 2014

Keywords:
Atmospheric transport
Plant pathogenic fungi
Fusarium head blight
Gaussian plume

ABSTRACT

Fusarium graminearum, causal agent of Fusarium head blight (FHB) of wheat and barley, is a devastating plant pathogen that may be transported through the atmosphere over long distances. A Gaussian dispersal model has been developed to predict the long distance transport of plant pathogens, but this model has not yet been experimentally validated for *F. graminearum*. Here, we compare the results of two release-recapture studies (conducted in 2011 and 2012) of *F. graminearum* from known field-scale sources of inoculum to those predicted by a Gaussian dispersal spore transport model. Dispersal kernel shape coefficients were similar for both results observed in the field and predicted by the model, with both being dictated by a power law function, indicating that turbulence was the dominant factor on a kilometer scale. Dispersal kernel predictions were also conducted using a more complicated Lagrangian Stochastic (LS) dispersal model. Dispersal kernel results were similar between the Gaussian and LS dispersal models. Model predictions had a stronger correlation with the number of spores being released when using a time varying q_0 emission rate ($r = 0.92$ in 2011 and $r = 0.84$ in 2012) than an identical daily pattern q_0 emission rate ($r = 0.35$ in 2011 and $r = 0.32$ in 2012). Temporal patterns of spore release and spore deposition in the field were not correlated (correlation coefficient of $r = -0.12$ for 2011 and $r = 0.45$ for 2012). The actual numbers of spores deposited from our known sources were monitored using microsatellites (short, repeated sequences of DNA), and were 3 and 2000 times lower than predicted if potential source strength, Q_{pot}, was equal to the actual number of spores released in 2011 and 2012, respectively. Differences between predicted and observed results in both years may have been due in part to variability in environmental conditions and spore release rates. This work provides a unique approach for validating a Gaussian spore transport model to predict the spore transport of *F. graminearum* over kilometer distances, and could be applied to other airborne plant pathogens in the future.

1. Introduction

Many plant pathogens are transported from a host to healthy crops through the atmosphere (Aylor, 1986, 1999; Aylor and Sutton, 1992; Aylor et al., 1982). *Phakospora pachyrhizi*, causal agent of Asian soybean rust (Krupa et al., 2006), and *Puccinia graminis* f. sp. tritici, causal agent of wheat stem rust (Stokstad, 2007), are two pathogens of recent concern that disperse their spores via the atmosphere (Krupa et al., 2006; Livingston et al., 2004; Pan et al., 2006; Singh et al., 2006, 2008a,b; Stokstad, 2007). *Fusarium graminearum* is another fungal plant pathogen that utilizes the atmosphere for spore transport (Maldonado-Ramirez et al., 2005; Schmale et al., 2006, 2012). This fungus is responsible for Fusarium head blight (FHB) of wheat and barley, which has resulted in more than $3 billion in crop losses in the United States over the past couple of decades (McMullen et al., 1997; Paulitz, 1999; Schmale III and Bergstrom, 2003). *Fusarium graminearum* produces deoxynivalenol (DON), a mycotoxin, that may contaminate food and feed and threaten the health of both humans and livestock (Snijders, 1990; Sutton, 1982).

Disease management for FHB has been a challenge for growers and farmers. Recent research has suggested that no-till practices have contributed to disease outbreaks by increasing the amount of potential inoculum sources (e.g., corn debris) on the soil surface (Dill-Macky and Jones, 2000; Keller et al., 2010, 2011). Additionally, fungicides have been found to have limited efficacy and must be

* Corresponding author. Tel.: +1 540 231 0733.
E-mail address: aprussin@vt.edu (A.J. Prussin II).

http://dx.doi.org/10.1016/j.agrformet.2014.12.009
0168-1923/

applied at the appropriate times and during specific environmental conditions (Bai and Shaner, 2004). It is easier to control disease and apply appropriate measures if the pathogen is detected early and the natural spread of the pathogen can be predicted (Gregory, 1961). Risk assessment tools have been developed for FHB (De Wolf et al., 2003; Del Ponte et al., 2009). The main considerations of these tools are environmental factors such as precipitation, relative humidity, and temperature to determine the relative risk of FHB. In addition to tools being able to predict FHB, tools have been developed to predict the amount of DON that might be produced based on environmental conditions (Schaafsma and Hooker, 2007). Although environmental factors are important for disease development of FHB on wheat and barley and mycotoxin production, the current risk assessment tools do not include the ability to predict the movement of *F. graminearum* spores from known inoculum sources. FHB risk assessment tools have the potential to be improved with new knowledge regarding spore transport from known inoculum sources.

A number of spore transport models have been developed based on an understanding of the atmospheric transport of plant pathogens (Aylor, 1986, 1999; Aylor and Flesch, 2001; Aylor and Sutton, 1992; Aylor et al., 1982). The atmospheric transport of plant pathogens can be described by the aerobiological processes of preconditioning, liberation, horizontal transport, deposition, impact, and infection (Isard et al., 2005). Models to predict the long distance transport of spores may assume a Gaussian distribution of spores (Aylor, 1999; Pasquill, 1976; Pasquill and Michael, 1977; Turner, 1970). The shape and width of the Gaussian distribution is dependent on atmospheric stability (Turner, 1970). Researchers have further developed these models to be specific for the long distance transport of plant pathogenic fungi (Aylor, 1986, 1999; Aylor and Sutton, 1992; Aylor et al., 1982). We consider long distance transport to be distances greater than or equal to 100 m from a source of inoculum. There are several factors in a Gaussian spore transport model necessary to predict the number of viable spores that will be deposited at any given location, including:

1. initial source strength
2. wind speed and direction
3. distance of healthy crops from the source
4. decrease in inoculum viability and spore loss due to solar radiation and deposition
5. dilution of spore plume due to turbulence

Lagrangian stochastic (LS) and Gaussian plume models are both popular choices for simulating the spread from a source on our scale of interest. Recently, an LS model was used to predict the transport of spores (sporangia) of the potato late blight pathogen, *Phytophthora infestans* up to 500 m from source fields (Aylor et al., 2011). The LS model was experimentally validated during two different field seasons with a series of aerial (unmanned aircraft) and ground-based (Rotorods) measurements (Aylor et al., 2011). Although LS models have been used to track the movement of plant pathogens (e.g., Aylor et al., 2011), they are complicated and require more computation time than a Gaussian transport model. Thus, Gaussian models may be more appropriate for farm use. Furthermore, a time averaged turbulent plume, of the kind produced by LS models, has been shown to be Gaussian over a sufficiently long period of time (Irwin et al., 2007), in particular, when concentrations are averaged over 30 min or longer, as is the case in our field experiments (Prussin II et al., 2014a).

Here, we extend the release-recapture concept of Aylor et al. (2011) to field studies of the long distance transport of *F. graminearum* assuming a Gaussian plume model for the dispersal of spores. Long distance transport models driven by a Gaussian distribution (1) can be calculated with limited meteorological data (wind speed, wind direction, rainfall rate, and solar radiation are the only variables needed), (2) are appropriate over the distances of interest (hundreds of meters) and expected to give reasonable results (Aylor, 1999), and (3) do not require numerical integration of differential equations, thus making them significantly less computationally intensive compared to LS models and therefore convenient to use. To verify the appropriateness of using a Gaussian dispersal model instead of an LS model to predict the long distance transport of a fungal plant pathogen, we created dispersal kernels predicted by both models for comparison.

The specific objectives of this study were to (1) model the long distance transport of *F. graminearum* using a previously described Gaussian spore transport model and meteorological data collected at our sampling site, and (2) validate the long distance transport model with release-recapture studies in the field over two growing seasons (Aylor, 1986, 1999; Aylor and Sutton, 1992; Aylor et al., 1982). *F. graminearum* spore dispersal kernels were derived from results predicted by the transport model and observed in the field and compared to determine the accuracy of the transport model. We hypothesized that the shape of the dispersal kernel for model and field observations would follow a power law, due to turbulence being the dominant factor of long distance transport over our distances of interest, between 100 and 1000 m (Aylor, 1999; Oboukhov, 1962). However, since the spore transport model is a simplification of a real-world cropping scenario and assumptions are made, we hypothesized that the spore transport model will overestimate the transport distance of spores and the number of spores that are deposited, as the model assumes a best case scenario in the environment for transport. Finally, we hypothesize that there will be greater accuracy in model predictions of spore deposition when time-resolved rather than time-averaged values of q_0, spore release rates, are used.

2. Materials and methods

2.1. Field experiments

Field studies were conducted at Virginia Tech's Kentland Farm in Blacksburg, Virginia from 26 April to 25 May 2011 and 9 April to 14 May 2012, as previously described (Prussin II et al., 2014a).

2.1.1. Field inoculation

Two hectares of winter wheat (untreated Southern States variety SS560) were planted in October 2010 for the 2011 field campaign and October 2011 for the 2012 field campaign. Mature, green corn stalks were collected in August 2010 and 2011 from corn fields at Virginia Tech's Kentland Farm in Blacksburg, VA and dried in a glass house for 6 months. The dried corn stalks were then cut into ~15 cm pieces and placed into 50 individual five-gallon steel buckets. Each of 50 buckets was filled approximately 2/3 full with cut corn stalks and autoclaved for 120 min. After the initial autoclaving step, the corn stalks were soaked in DI water overnight, the water was then removed, and the corn stalks were autoclaved again for 120 min. The autoclaved corn stalks were then inoculated with colonized agar pieces of *F. gramineaerum* isolate Fg_Va_GPS13N4_3ADON (hereafter referred to as FGVA4) from five 100 mm diameter Petri dishes that had been cultured on ¼-strength PDA for 12 days. The buckets containing the inoculated corn stalks were stored at ambient room temperature for approximately 10 weeks to allow the fungus to colonize the corn stalks.

A plot area of 3716 m^2 (0.372 ha) of wheat was subdivided into 100 square plots (10 rows of 10 plots, 6.096 m (20 ft) × 6.096 m (20 ft)). Field inoculations were performed on 2 May 2011 (season 1) and 16 April 2012 (season 2) by releasing corn stalks from each

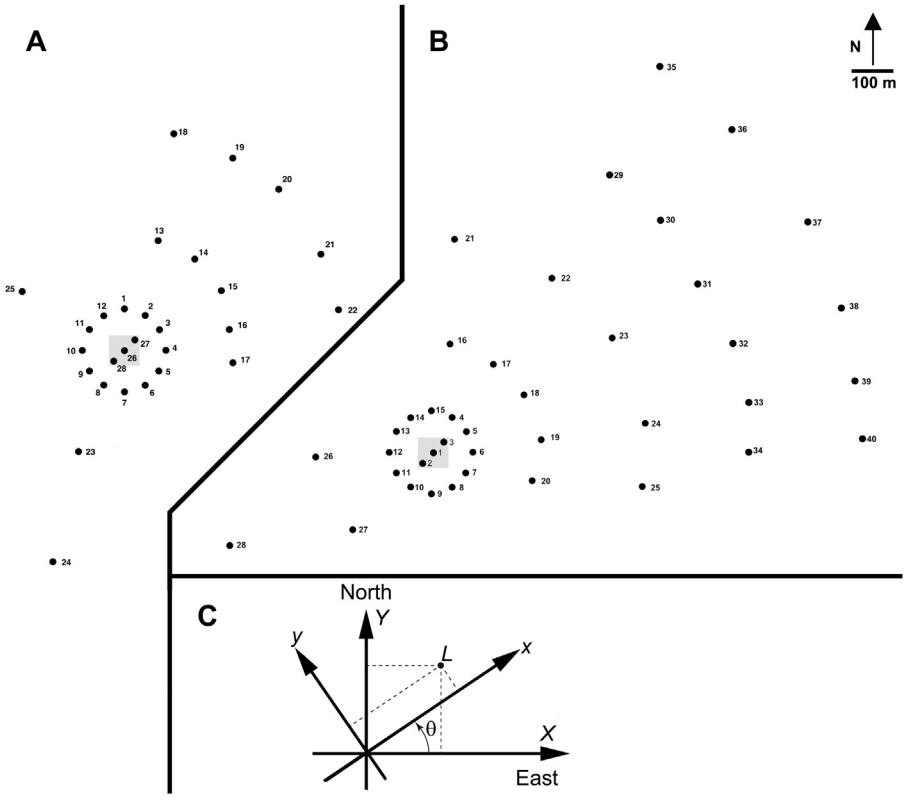

Fig. 1. Collection locations at different distances from clonal 3716 m^2 (0.372 ha) sources of inoculum (gray squares) of *Fusarium graminearum* at Virginia Tech's Kentland Farm in Blacksburg, VA for the 2011 (A) and 2012 (B) field campaigns. In 2011, collection sites 1–12 were 100 m from the center of the source, sites 13–17, 23, and 25 were 250 m from the center of the source, sites 18–22 and 24 were 500 m from the center of the source, and sites 26–28 were in the source (site 26 was in the center of the source). In 2012, collection sites 1–3 were in the source, sites 4–15 were 100 m from the center of the source, sites 16–20, 26, and 27 were 250 m from the center of the source, sites 21–25 and 28 were 500 m from the center of the source, sites 29–34 were 750 m from the center of the source, and sites 35–40 were 1000 m from the center of the source. The location of these devices was informed based on historical wind data as reported by Prussin et al. (2014a). An example of the rotating matrix is shown (C).
Figure modified from Prussin et al. (2014a).

of the 50 buckets into 50 of the subplots in a checkerboard pattern (stalks from one bucket were used for each of the subplots).

2.1.2. Sample collection and identification

As described previously, a series of ground-based collection devices were placed in the source and at distances of 100, 250, and 500 m from the center of the inoculated field in 2011, and in the source and at 100, 250, 500, 750, and 1000 m, from the center of the inoculated field in 2012 (Fig. 1) (Prussin II et al., 2014a). The location of these devices was informed based on historical wind data as reported by Prussin et al. (2014a). The ground-based collection devices consisted of a Petri plate containing a Fusarium selective medium (FSM) placed atop a 1 m wooden stake to collect viable spores of *Fusarium*. The FSM was prepared as previously described (Schmale III et al., 2006). In 2011, spore deposition samples were continuously collected in the field during the day (0700–1900) and night (1900–0700) for 14 consecutive days (12–25 May 2011), corresponding to the presence of perithecia on the corn stalks. In 2012, spore deposition samples were continuously collected in the field during the day, specifically morning (0700–1100) and night (1900–0700) for 19 consecutive days (26 April–14 May 2012), corresponding to the presence of perithecia on the corn stalks.

After each sampling period, exposed Petri plates were immediately removed from the field, covered, and placed in small plastic boxes for transport to the laboratory. The plates were incubated for 7–10 days in the laboratory at ambient room temperature and the number of *Fusarium* colonies (distinct white, fluffy colonies approximately 15 mm in diameter) collected at each location during each sampling period was recorded. Up to five *Fusarium* colonies from each plate were randomly selected and sub-cultured to Petri plates containing 1/4-strength PDA, in 2011. In 2012, the number of *Fusarium* samples further sub-cultured and studied was increased to ten colonies per plate. Colonies producing red, pink, or yellow mycelia characteristic of *F. graminearum* and containing only macroconidia on ¼-strength PDA, were single-spored onto additional plates. Single-spored cultures were placed in 20% glycerol and stored at −80 °C. Single-spored isolates identified as *F. graminearum* were grown in 100 mL of 1/4-strength PD broth on a shaker at 100 rpm for 5–7 days at ambient room temperature. Harvesting of mycelia and extraction of DNA were conducted following previously published methods (Keller et al., 2010, 2011). Three microsatellites were used to genotype all *F. graminearum* isolates from the field collection (Vogelgsang et al., 2009). *F. graminearum* samples having identical allelic sizes as the released clone, FGVA4, at all three microsatellite locations were identified as being the released clone as previously described (Prussin II et al., 2014a).

Since only a subset of all the *Fusarium* colonies were sub-cultured and analyzed for the released clone, to estimate the total number of the released clone recaptured on each sampling plate, the fraction of sub-cultured isolates that were identified as the released clone was multiplied by the total number of *Fusarium* colonies.

2.1.3. Meteorological data

Meteorological data (wind speed, wind direction, solar radiation, and rainfall rate) used in the transport model was obtained from the Virginia Agricultural Experimental Station Mesonet weather station located at Kentland Farm. The weather station's

Table 1
Constants used to determine Gaussian plume spread parameters σ_y (m) and σ_z (m).

	Atmospheric stability class					
Coefficient	*A*	*B*	*C*	*D*	*E*	*F*
I_y	−1.104	−1.634	−2.054	−2.555	−2.754	−3.143
J_y	0.9878	1.0350	1.0231	1.0423	1.0106	1.0148
K_y	−0.0076	−0.0096	−0.0076	−0.0087	−0.0064	−0.0070
I_z	4.679	−1.999	−2.341	−3.186	−3.783	−4.490
J_z	−1.7172	0.8752	0.9477	1.1737	1.3010	1.4024
K_z	0.2770	0.0136	−0.0020	−0.0316	−0.0450	−0.0540

Adapted from Seinfeld and Pandis (2006).

sensors were approximately 2 m above ground level. The weather station was located approximately 250 m northwest from the center of our source of inoculum in 2011, and approximately 350 m northwest from the center of our source of inoculum in 2012. Weather data was recorded at 15 min intervals.

2.2. Model

We used a universal transport model for plant pathogens described by Aylor (1999) to compare model predictions to field observations, as shown below.

2.2.1. Gaussian plume model

The following assumptions were made for our model: (1) a continuous release of *F. graminearum* ascospores from the source of inoculum, (2) a point source of inoculum, (3) the long distance transport of spores from a known source of inoculum followed a Gaussian plume distribution and is represented by the following equation (Aylor, 1999; Gifford Jr, 1968):

$$C(x,y,z) = \frac{q_0}{\pi\sigma_y\sigma_z U_c}\exp\left(\frac{-y^2}{2\sigma_y^2}\right)\exp\left(\frac{-z^2}{2\sigma_z^2}\right) \quad (1)$$

distances x, y, and z correspond to the horizontal distance of the sampling location downwind from the center of the source of inoculum, distance away from the centerline of the spore plume, and the sampling height, respectively. Wind speed is represented by U_c and measured in m s^{-1} and spore release rate is given by q_0. Standard deviations of the spread of the plume in the y and z directions are given by σ_y (m) and σ_z (m), respectively, which are functions of sampling distance downwind, x (m), and can be calculated using the following equations (Turner, 1970):

$$\sigma_y(x) = \exp[I_y + J_y \ln x + K_y(\ln x)^2] \quad (2a)$$

$$\sigma_z(x) = \exp[I_z + J_z \ln x + K_z(\ln x)^2] \quad (2b)$$

where I_y, J_y, K_y, I_z, J_z, and K_z are constants that depend on the atmospheric stability class, as shown in Table 1 (Gifford Jr, 1961, 1968; Pasquill, 1976; Turner, 1970). Atmospheric stability was calculated using Pasquill stability classes (Turner, 1970). There are six stability classes; Classes A, B, C, D, E, F corresponding to extremely unstable, moderately unstable, slightly unstable, neutral, slightly stable, and moderately stable, respectively. Atmospheric stability class was calculated as a function of solar radiation and wind speed as shown in Table 2.

We note that in general, U_c, q_0, σ_y, and σ_z vary in time, and the greatest uncertainty lies in estimating $q_0(t)$. Previous work has suggested the uncertainty in estimating $q_0(t)$ is between a factor of 100 and 1000 (Aylor, 1986). We will provide two assumptions to estimate $q_0(t)$, discussed below.

2.2.2. Distance of sampling location from center of spore plume

Each sampling location had fixed (*X*,*Y*) coordinates, where *X* and *Y* are the eastward and northward distances, respectively, of the sampler with respect to the center of the source. For modeling, the relevant position is (x, y) (see Fig. 1C). To calculate the x and y distances used in the model the following equations were used:

$$x = X\cos\theta + Y\sin\theta \quad (3a)$$

$$y = Y\cos\theta - X\sin\theta \quad (3b)$$

where θ is the angle of the wind heading, as shown in Fig. 1C. The values of X and Y were calculated using GPS waypoints for each sampling location in 2011 (Fig. 1A) and 2012 (Fig. 1B).

2.2.3. Spore loss and decrease in inoculum viability

Eq. (1) assumes no spores are being lost during transport. The major factor that contributes to the physical loss of spores is deposition, and the major factor that contributes to a decrease in inoculum viability is solar radiation. Though non-viable (dead) spores can be transported through the atmosphere, only viable spores are considered in the model since they have the ability to cause disease. The fraction of spores surviving exposure to solar radiation is given by the following expression (Aylor, 1999),

$$f_s = \exp\left(\frac{-Ix}{I_* t_* U_c}\right) \quad (4a)$$

where I is solar radiation (W m^{-2}) and I_*t_* is the dose of radiation to kill a fraction $1 - 1/e$ of the spores. There is a wide range of I_*t_* values for fungal spores ranging from less than 1 MJ m^{-2} to over 35 MJ m^{-2} (Aylor, 1999). The two extreme I_*t_* values were examined (1 MJ m^{-2} and 35 MJ m^{-2}), and we determined that on the scale we are modeling transport (<1 km), I_*t_* was negligible for spore loss. While there are some preliminary estimates for I_*t_* for *F. graminearum* (Nita et al., 2008), for the purposes of our model, an I_*t_* of 20 MJ m^{-2} was assumed as this is in the range of reported I_*t_* values. Additionally, *Venturia inaequalis*, another ascomycete, has an I_*t_* value of 21 MJ m^{-2} (Aylor and Sanogo, 1997).

Deposition can occur either due to the natural settling of spores, known as dry deposition, or because of spore washout due to rainfall, known as wet deposition. The fraction of spores that are not

Table 2
Atmospheric stability class as a function of solar radiation and wind speed.[e]

Wind speed (m s^{-1})	Daytime Incoming solar radiation			Nighttime[d]
	Strong[a]	Moderate[b]	Slight[c]	
<2	*A*	*B*	*B*	*F*
2–3	*B*	*B*	*C*	*E*
3–5	*B*	*C*	*C*	*D*
5–6	*C*	*D*	*D*	*D*
>6	*C*	*D*	*D*	*D*

Table adapted from Turner (1970).
[a] Solar radiation >700 W m^{-2}.
[b] Solar radiation 350–700 W m^{-2}.
[c] Solar radiation <350 W m^{-2}.
[d] No solar radiation present.

removed from the atmosphere by either wet or dry deposition is given by the following equation (Aylor, 1999):

$$f_d = \exp\left(\frac{-(\Gamma_w + \Gamma_d)x}{U_c}\right) \tag{4b}$$

Γ_w and Γ_d are the effective rates (s^{-1}) for wet and dry deposition, respectively, and can be represented as (Aylor, 1999; Aylor and Sutton, 1992):

$$\Gamma_w = 0.000272R^{0.7873} \tag{4c}$$

$$\Gamma_d = \sqrt{\frac{2}{\pi}}\left(\frac{v_s}{x}\right)\int_{x_0}^{x}\left[\frac{dx}{\sigma_z(x)}\right] = \sqrt{\frac{2}{\pi}}\left(\frac{v_s}{x}\right)\left(\frac{\sqrt{\pi}\exp(((J_z-1)^2/4K_z)-I_z)(1+\mathrm{erf}((2K_z\ln(x)+J_z-1)/2\sqrt{K_z}))}{2\sqrt{K_z}}\right) \tag{4d}$$

where R is the rain fall rate given in mm h^{-1} and v_s is the settling velocity of *F. graminearum* ascospores. J_z and K_z are empirical constants used to calculate the spread of the plume as described above. The settling velocity of *F. graminearum* ascospores is approximately 1.27 mm s^{-1} (Schmale III et al., 2005; Trail et al., 2005).

The number of spores remaining airborne and not lost due to solar radiation at some distance downwind from the center of the source of inoculum, x, and atmospheric wind speed, U_c, can be represented as (Aylor, 1999):

$$q\left(\frac{x}{U_c}\right) = f_s f_d q_0 \tag{4e}$$

where q_0 is the initial spore release rate at $x = 0$, the center of the inoculum source. The concentration of viable *F. graminearum* spores at any distance from the center of the source of inoculum (taking into account spore loss due to deposition and solar radiation) can be determined by substituting $q(x/U_c)$ for q_0 in (1), giving:

$$C(x,y,z) = \frac{q(x/U_c)}{\pi\sigma_y\sigma_z U_c}\exp\left(\frac{-y^2}{2\sigma_y^2}\right)\exp\left(\frac{-z^2}{2\sigma_z^2}\right) \tag{4f}$$

2.2.4. Number of spores deposited

The number of *F. graminearum* spores deposited at each sampling location can be calculated by determining the deposition flux. For simplicity, it is assumed that every ascospore that intercepted the Petri dish became deposited and produced a colony-forming unit. Deposition velocity is given by (Aylor and Sutton, 1992):

$$v_x = v_d + v_w \tag{5a}$$

where v_d and v_w are the velocities for dry and wet deposition, respectively, and can be represented as (Aylor and Sutton, 1992):

$$v_d = v_s \tag{5b}$$

$$v_w = 1.25\Gamma_w\sigma_z \tag{5c}$$

Finally, the total number of spores deposited on a horizontal dish of surface area S, over a sampling duration T, at any given location (x, y, z), is

$$D = C(x,y,z)v_x ST \tag{5d}$$

2.2.5. Estimation of q_0

One of the most difficult model parameters to estimate is the time dependent spore release rate for the source, $q_0(t)$ (Aylor, 1986). In previous work, Prussin et al. (2014b) quantified Q_{pot}, or the maximum potential number of *F. graminearum* ascospores released from our plot throughout the entire sampling period. In order to estimate q_0 we used a combination of spore capture data collected by a volumetric spore sampler (Quest) and knowledge of Q_{pot}. The potential source strength, Q_{pot}, of our one acre artificially inoculated plot was estimated to be approximately 3.7 billion ascospores (Prussin II et al., 2014b). The relative number of spores released each hour was determined and combined with Q_{pot} to give an estimated number of spores being released from the one acre plot each hour. The relative number of spores being released was quantified from one volumetric spore sampler placed in the center of the inoculated field and spore release was assumed to be spatially uniform throughout the entire field. Since the model was completed with a time resolution of 15 min, we divided the number of spores being released each hour by 4 to get an input value for q_0 for each 15 min interval. This $q_0(t)$ we refer to as time varying ${q_0}^{tv}(t)$. In 2011, we only had spore release data for the second week of field sampling (19–25 May 2011) and therefore could not use ${q_0}^{tv}(t)$ for the first week of sampling (12–19 May 2011). To get an estimate of $q_0(t)$ which could include the first week of sampling, an identical daily pattern ${q_0}^{idp}(t)$ was calculated for each hour interval in a day based on the average observed pattern (Fig. 2) (e.g., spore release was assumed to be the same at 0100 everyday, the same at 0200 everyday, etc.) (Prussin II et al., 2014b). Identical daily pattern ${q_0}^{idp}(t)$ was used for the entire sampling periods in both 2011 and 2012. Additionally, we compared the results of using either identical daily pattern ${q_0}^{idp}(t)$ or time varying ${q_0}^{tv}(t)$ in the model.

2.3. Comparison of model results to field results

Spore deposition observed in the field and predicted by the model was analyzed for both 2011 and 2012. In 2012 and the second week of 2011 (19–25 May 2011), q_0 was estimated using time varying ${q_0}^{tv}(t)$. Additionally, for the entire sampling periods in 2011 and 2012 q_0 was estimated using the identical daily pattern ${q_0}^{idp}(t)$. Note that if we approximate the deposition as occurring exactly downwind (i.e., $y = z = 0$), (**5d**) has the functional form of a dispersal kernel,

$$D(x) = ax^b e^{-cx} \tag{6a}$$

where

$$a = \frac{{q_0}^{ave} v_x ST}{\pi U_c e^{J_y + I_z}} \tag{6b}$$

$$b = -(J_y + J_z) \tag{6c}$$

$$c = \frac{I}{I_* t_* U_c} + \frac{\Gamma_w + \Gamma_d}{U_c} \tag{6d}$$

Thus, curve-fitting via non-linear regression analysis allows us to estimate a, b, and c. If other factors are known, this provides an independent means to approximate the average release rate ${q_0}^{ave}$. As the Gaussian point source model is a better approximation outside the inoculated field, samples that were in the source of inoculum were not included in the analyses.

The model was evaluated by plotting the measured number of spores deposited in the field at each location for each sampling period against the corresponding model prediction for that location and time. Additionally, model performance was evaluated using the mean bias (B_{MB}), mean normalized bias (B_{MNB}), mean absolute gross error (E_{MAGE}), and mean normalized gross error (E_{MNGE}). These values report whether the model tends to over-predict or under-predict the observations and how large the differences are.

3. Results

3.1. Dispersal kernels

Overall dispersal kernels were estimated for the entire sampling period (~2 weeks) from results observed in the field and predicted

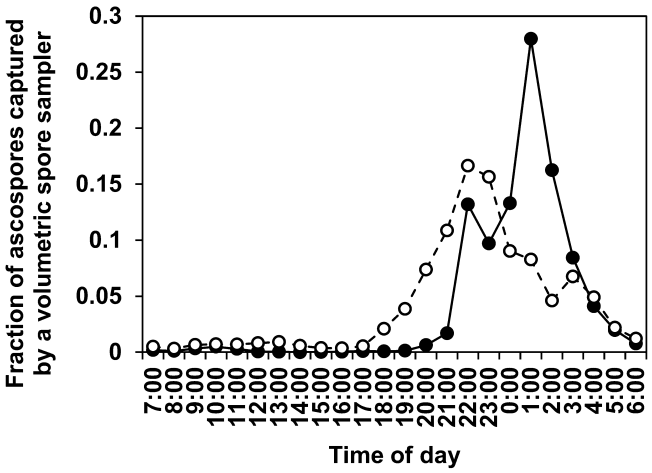

Fig. 2. Fraction of ascospores released and captured by a volumetric spore sampler in the center of a one-acre wheat field inoculated with FGVA4 during different times of the day in 2011 (closed circles) and 2012 (open circles).
Figure adapted from Prussin II et al. (2014b).

by the model. These are shown in Fig. 3, where the total deposition shown is normalized by the value at 100 m, i.e., $D(100\,\text{m}) = 1$. In 2011, the results obtained in the field at 500 m are overlying the results predicted by the Gaussian model. In 2012, no data were collected in the field 250 or 1000 m from the center of the source of inoculum. For comparison, dispersal kernels using a LS prediction tool are also presented in Fig. 3. A description of the LS model is presented in Appendix A. Dispersal kernels were created by fitting the deposition data to the functional form given by Eq. (6a). The b and c parameters are given in Table 3 for 2011 using the identical daily pattern ${q_0}^{idp}(t)$ in the model, 2011 using time varying ${q_0}^{tv}(t)$ in the model, 2012 using time varying ${q_0}^{tv}(t)$ in the model, and 2012 using the identical daily spore release pattern for ${q_0}^{idp}(t)$ in the model. It is expected that the LS model becomes approximately a Gaussian model over the distances we considered (greater than 100 m), indicating that a Gaussian model is appropriate to study the long distance transport of a fungal plant pathogen (Irwin et al., 2007). Both the Gaussian model and LS model showed similar predicted dispersal kernel values for spore transport, however the magnitude of b was consistently smaller for the Gaussian model compared to the LS model, suggesting the LS model overestimates the role of turbulence over the distances considered. It is noteworthy that both the Gaussian and LS models show parameter b as the dominant factor in determining the shape of the dispersal kernel on the scale studied. A dominant b parameter indicates a dispersal kernel is governed by a power function and thus turbulent diffusion is the main factor in transport; while a dominant c coefficient indicates the dispersal kernel is governed by an exponential function and thus spore loss from solar radiation and deposition (wet and dry) are the dominating factors in transport (Aylor, 1999). The results we obtained indicate that, on the scale we studied (<1 km), turbulence was the dominant mechanism of spore transport and spore loss from deposition and solar radiation were negligible.

In 2011, the coefficient for the b variable was smaller for the results observed in the field than predicted by the model for both time varying ${q_0}^{tv}(t)$ and identical daily pattern ${q_0}^{idp}(t)$ inputs. This suggests that the model over-predicted the 'fat-tail' of the dispersal

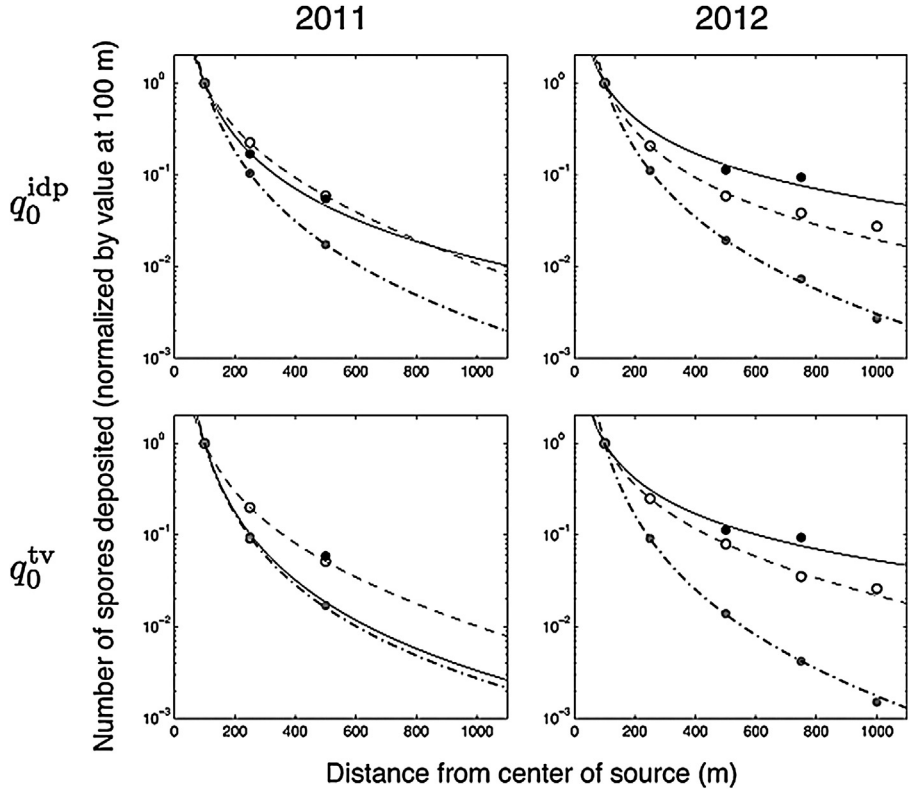

Fig. 3. Dispersal kernels for *F. graminearum* spores released from a known source of inoculum predicted by the Gaussian model (dashed line), LS model (dashed-dot line) and observed in the field (solid line) for 2011 (left panel) and 2012 (right panel) assuming identical daily spore release pattern ${q_0}^{idp}$ (top) and time varying spore release ${q_0}^{tv}$ (bottom). In 2011, the results obtained in the field (solid-circle) at 500 m are overlying the results predicted by the Gaussian model (open-circle.) For model comparison, only the second week (19–25 May) of results observed in the field is shown for 2011 ${q_0}^{tv}$. In 2012, no data were collected in the field 250 m or 1000 m from the center of the source of inoculum. For the plots, total deposition, D, is normalized to samples collected 100 m from the source of inoculum. Open circles and gray circles are individual data points generated by the Gaussian model and LS model, respectively, at varying distances while solid circles are data points collected in the field at varying distances.

Table 3
Coefficient values for the observed and predicted dispersal kernels of *F. graminearum* spores from a known source of inoculum in 2011 and 2012.[a]

q_0 Input	Year		b[c]	c[c]	R^2	Estimated[d]	
						b	c
Identical daily spore release pattern	2011	Observed	−1.91	0	0.99	−2.04	0.004
		Gaussian	−1.40	0.0015	0.99	–	–
		LS	−2.37	0	0.99	–	–
Time varying spore release	2011	Observed[b]	−2.48	0	0.99	−2.06	0.004
		Gaussian	−1.58	0	0.99	–	–
		LS	−2.56	0	0.99	–	–
Identical daily spore release pattern	2012	Observed	−1.28	0	0.99	−2.06	0.018
		Gaussian	−1.71	0	0.99	–	–
		LS	−2.32	0	0.99	–	–
Time varying spore release	2012	Observed	−1.28	0	0.99	−2.06	0.018
		Gaussian	−1.40	0.0007	0.99	–	–
		LS	−2.51	0	0.99	–	–

[a] Dispersal kernels were fitted to the following function: $D = ax^b e^{-cx}$, where x is distance from the center of the source of inoculum.
[b] Only included the second week of field data (19–25 May 2011) and model was only run for this time period.
[c] Calculated from dispersal kernel.
[d] b and c coefficients were estimated using Eqs. (6c) and (6d) with collected meteorological data from the field. Coefficients were only estimated for the observed results in the field.

kernel and the distance the spores would be transported. However, in 2012, the coefficient for the b variable was slightly larger for the results observed in the field than predicted by the model, suggesting the model under-predicted the 'fat-tail' of the dispersal kernel and the distance spores can be transported.

An estimate of the average spore release rate, ${q_0}^{ave}$, and estimated source strength, Q_{est}, were obtained from the curve-fitted value of a for the dispersal kernel. Using Eq. (6b), we considered the average wind speed, I_y, I_z, downward flux, sampling surface area, and total sampling time (T_{tot}) during the sampling period, and solved for the average spore release rate, ${q_0}^{ave}$. To obtain the estimated source strength, we used $Q_{est} = {q_0}^{ave}\ T_{tot}$ as calculated for 2011 and 2012 (Table 4). In 2011, the average ${q_0}^{ave}$ was calculated to be 2850 spores s^{-1}, which yielded a Q_{est} of approximately 3.2 billion ascospores released from the inoculated field during the sampling period. In 2012, the average ${q_0}^{ave}$ was calculated to be 1.35 spores s^{-1}, which yielded a Q_{est} of approximately 2.1 million ascospores. The potential source strength of the field was estimated to be 3.7 billion ascospores (Prussin II et al., 2014b). Thus, approximately 86% of the total number of ascospores potentially present were released during our sampling period in 2011; while only 0.06% of the total number of ascospores potentially present were released during our sampling period in 2012. A potential reason for the differences in spore release between 2011 and 2012 might be linked to environmental conditions and is further discussed by Prussin II et al. (2014b).

Table 4
Estimation of average ${q_0}^{ave}$ and total source strength for 2011 and 2012.

Parameter	2011	2012
a[a]	867,887 spores	645 spores
S[b]	0.00567 m^2	0.00567 m^2
T_{tot}[c]	1,123,200 s	1,533,600 s
U_c[d]	1.55 m s^{-1}	1.44 m s^{-1}
I_y[e]	−2.33	−2.34
I_z[e]	−2.88	−2.94
$f(x)$[f]	0.00127 m s^{-1}	0.00127 m s^{-1}
${q_0}^{ave}$[g]	2850 spores s^{-1}	1.35 spores s^{-1}
Q_{est}[h]	3.2×10^9 spores	2.1×10^6 spores

[a] Calculated from dispersal kernel fit to Eq. (6a) for field deposition data.
[b] Surface area of sampling dish collecting deposition samples.
[c] Total sampling time for collecting deposition.
[d] Average wind speed.
[e] Average coefficient calculated from Table 1.
[f] Average downward spore flux.
[g] Average spore release rate from field calculated using Eq. (6b).
[h] Estimated total source strength during sampling period calculated from ${q_0}^{ave}$ and T_{tot}.

3.2. Comparison of field observations to model predictions

The number of *F. graminearum* spores released from the inoculated field and deposited compared to the number of spores predicted to be deposited by the model is shown in Fig. 4. In 2011, using the identical daily pattern ${q_0}^{idp}(t)$ in the model, the majority of the points fall above the diagonal line, indicating an over-prediction of the actual number of spores being deposited; however when time varying ${q_0}^{tv}(t)$ was used in the model, points fall closer to the diagonal line indicating better agreement between the model and results observed in the field. More data points were observed when using identical daily pattern ${q_0}^{idp}(t)$, because we were able to include the entire sampling period (12 May–25 May 2011) in our analysis, rather than just the second week of sampling (19 May–25 May 2011) which could only be used when using time varying ${q_0}^{tv}(t)$ in the model (there was no volumetric spore sampler data for 12 May–19 May 2011). Using the ${q_0}^{ave}$ from the dispersal kernel analysis above, we can consider an a posteriori, or corrected, version of the time-varying model which uses a re-scaled $q_0(t)$ based on the estimated number of spores released. The corrected spore release model is shown in the bottom panel. In 2012, when either time varying ${q_0}^{tv}(t)$, identical daily pattern ${q_0}^{idp}(t)$, or corrected q_0 was used in the model, all the data points fell above the horizontal line indicating an over-prediction of the model when compared to field observations.

Model performance was evaluated using the mean bias (B_{MB}), mean normalized bias (B_{MNB}), mean absolute gross error (E_{MAGE}), and mean normalized gross error (E_{MNGE}). The results of these analyses are shown in Table 5. The E_{MNGE} results indicate that for 2011 the model over-predicted the number of spores that would be deposited on any given sampler by an average of about 3 times and 150 times when either time varying or identical daily patterns were used as the model input for $q_0(t)$, respectively. In 2012, the E_{MNGE} results indicated that the model over predicted the number of spores that would be deposited on any given sampler by about 2000 times and 630 times when either time varying or identical daily patterns were used as the model input for $q_0(t)$, respectively. However, for the corrected spore release rate, the B_{MNB} and E_{MNGE} are much closer to 100%.

In 2011, a daily comparison was made between the number of spores released from the field that were captured by the volumetric spore sampler in the center of the field (Fig. 5A), the sum of the

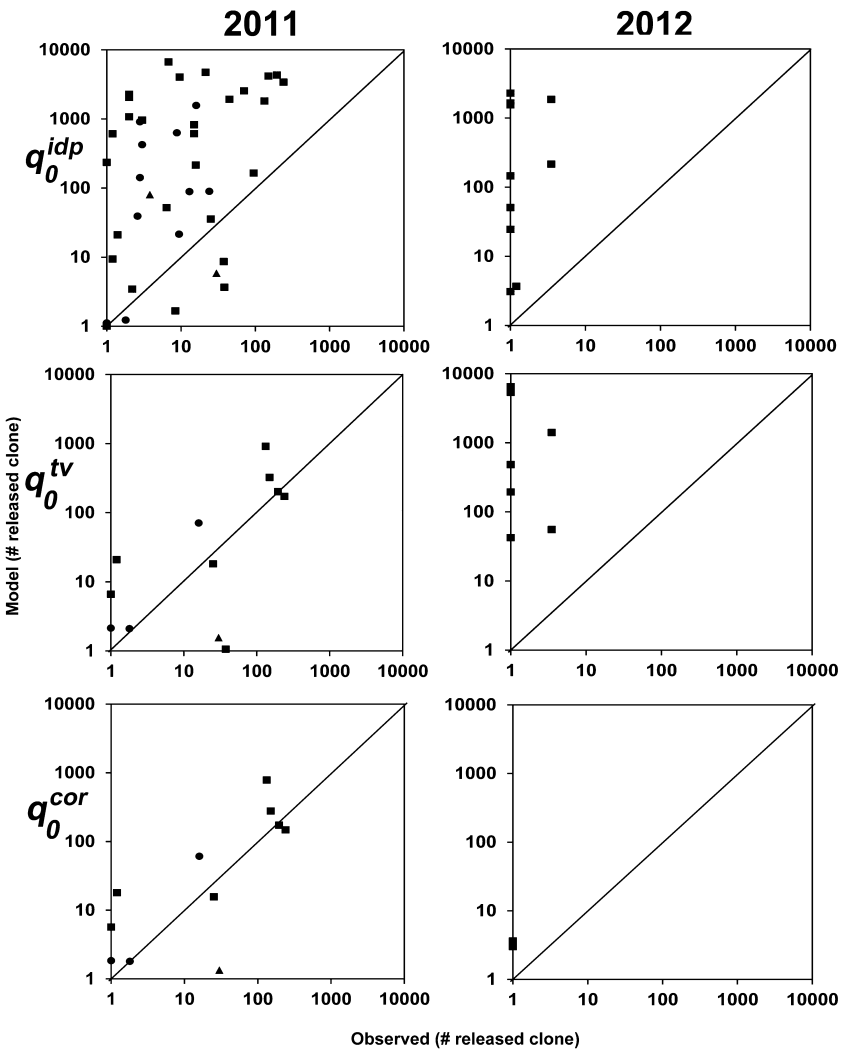

Fig. 4. Comparison of the number of *F. graminearum* spores deposited that were observed in the field and predicted by the model in 2011 (left panel) and 2012 (right panel) assuming identical daily spore release pattern $q_0{}^{idp}$ (top), time varying spore release $q_0{}^{tv}$ (middle), and corrected release $q_0{}^{cor}$ (bottom) for distances of 100 m (square), 250 m (circle), and 500 m (triangle) from the source of inoculum. In order to be included in the graph, a spore must have been deposited both in the field and have been predicted to be deposited by the model. This information is shown in Fig. S1. Data points that fall on the diagonal line of each graph had agreement between the results predicted by the model and observed in the field. Data points above the line were over-predicted by the model and those below the line were under-predicted by the model.

number of spores released from the field that were recaptured at all the deposition locations (Fig. 5B), the model prediction assuming a time varying $q_0{}^{tv}(t)$ input (Fig. 5C), the model prediction assuming an identical daily pattern $q_0{}^{idp}(t)$ input (Fig. 5D), and rainfall (Fig. 5E). There were no data for spore release between May 12 (day) and May 19 (day), which is the reason there are no results for the model assuming an time varying release $q_0{}^{tv}(t)$ input during the same time period. There was poor agreement between field deposition pattern and model predictions assuming both time varying release $q_0{}^{tv}(t)$ input ($r = -0.15$) and an identical daily pattern $q_0{}^{idp}(t)$ input ($r = 0.14$). There was no discernible agreement between the spore release pattern and the field deposition pattern ($r = -0.12$) or the model assuming an identical daily pattern $q_0{}^{idp}(t)$ input ($r = 0.35$). A strong correlation was observed between

Table 5
Statistical metrics to compare model performance to results observed in the field[a] in 2011[b] and 2012[c].

Metric	2011			2012		
	Time varying spore release[d]	Identical daily spore release pattern[e]	Corrected spore release rate	Time varying spore release[d]	Identical daily spore release pattern[e]	Corrected spore release rate
B_{MB} (spores)	75	1080	38	2000	778	0.66
B_{MNB}	261%	15,200%	145%	185,000%	63,000%	66%
E_{MAGE} (spores)	98	1090	55	1970	778	0.66
E_{MNGE}	302%	15,200%	166%	182,000%	63,000%	66%

[a] 3716 m^2 plot was inoculated with a single clonal isolate of *Fusarium graminearum*.
[b] The 2011 field season consisted of 14 consecutive days of sampling (12–25 May 2011).
[c] The 2012 field season consisted of 19 consecutive days of sampling (26 April–14 May 2012).
[d] Model was performed using time varying spore release as an input for q_0.
[e] Model was performed using identical daily spore release pattern as an input for q_0.

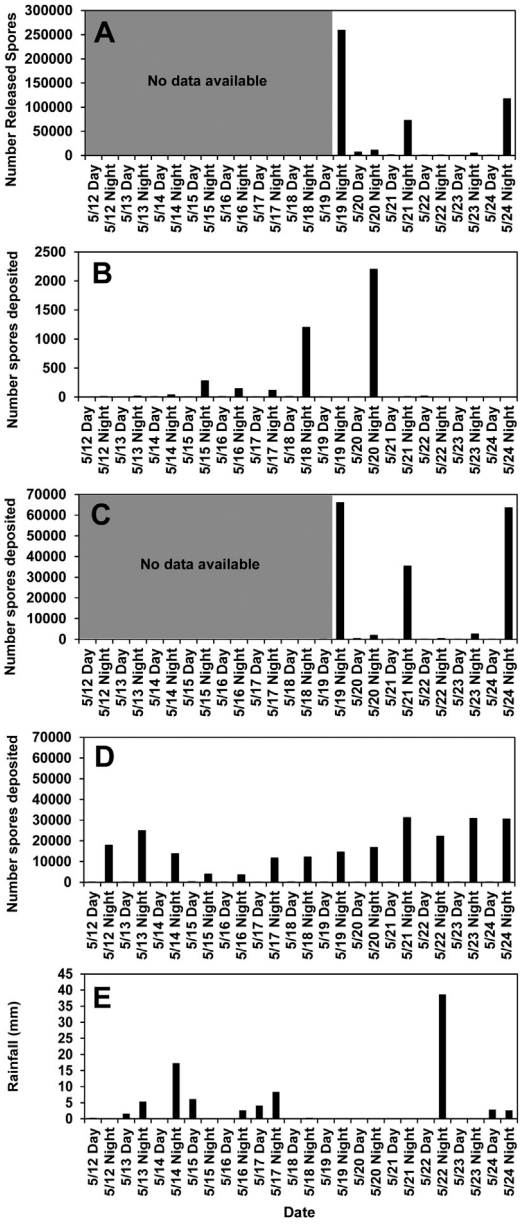

Fig. 5. Comparison between the number of *F. graminearum* spores released and captured by the volumetric spore sampler in the center of the inoculated field (A), number of spores released from the source deposited in the field (B), number of spores predicted to be deposited using time varying spore release as the input for q_0 in the model for 2011 (C), number of spores predicted to be deposited using identical daily spore release pattern as the input for q_0 in the model (D), and total rainfall during each sampling period (E).

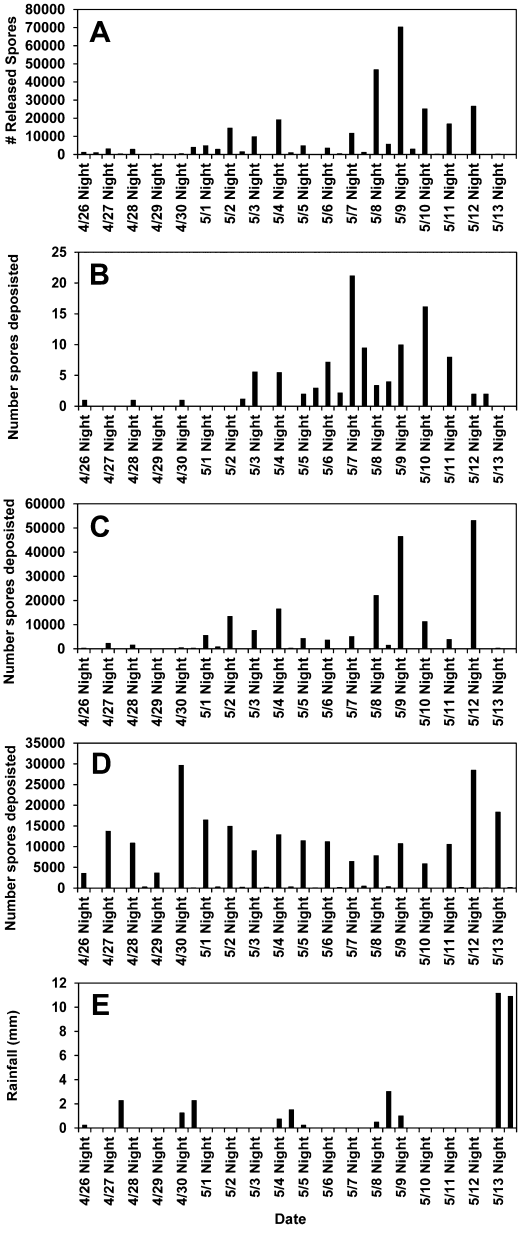

Fig. 6. Comparison between the numbers of *F. graminearum* spores released and captured by the volumetric spore sampler in the center of the inoculated field (A), number of spores released from the source deposited in the field (B), number of spores predicted to be deposited using time varying spore release as the input for q_0 in the model for 2012 (C), number of spores predicted to be deposited using time varying spore release as the input for q_0 in the model for 2012 (C), and total rainfall during each sampling period (E).

the spore release pattern and the model assuming time varying release $q_0{}^{tv}(t)$ input ($r = 0.92$). This was expected, since the source strength input in the model was based on data collected in the field. Interestingly, there was no discernible agreement between the patterns of field deposition and rainfall ($r = -0.12$). On the scale studied (<1 km), rainfall does not appear to have a significant influence on spore deposition. This result is consistent with the model (assuming a time varying release $q_0{}^{tv}(t)$ input) predicting no relationship between spore deposition and rainfall ($r = -0.15$).

In 2012, a daily comparison was made between the number of spores released from the field that were captured by the volumetric spore sampler in the center of the field (Fig. 6A), the sum of the number of spores released from the field that were recaptured at all the deposition locations (Fig. 6B), the model prediction assuming a time varying $q_0{}^{tv}(t)$ input (Fig. 6C), the model prediction assuming an identical daily pattern $q_0{}^{idp}(t)$ input (Fig. 6D) and rainfall (Fig. 6E). There was poor agreement between the field deposition pattern and model predictions, assuming both time varying release $q_0{}^{tv}(t)$ input ($r = 0.27$) and an identical daily pattern $q_0{}^{idp}(t)$ input ($r = 0.08$). There was no discernible agreement between the spore release pattern and the field deposition pattern ($r = 0.45$) or the model assuming an identical daily pattern $q_0{}^{idp}(t)$ input ($r = 0.31$). A strong correlation was observed between the spore release pattern and the model, assuming time varying release $q_0{}^{tv}(t)$ input ($r = 0.84$). This was expected, since the source strength input in the model was based on data collected in the field. As in 2011, during the 2012 field campaign rainfall does not appear to have a significant influence on spore deposition in the field ($r = -0.17$), which is

consistent with the model (assuming time varying release $q_0{}^{tv}(t)$ input) predicting no relationship between spore deposition and rainfall ($r = -0.10$).

4. Discussion and conclusions

In this study, we compared results predicted by a simple Gaussian long distance transport model to results observed in release-recapture field studies conducted over two years for *F. graminearum*. We used a previously described transport model for plant pathogenic fungi in our study with parameters unique to *F. graminearum* (Aylor, 1986, 1999; Aylor and Sutton, 1992; Aylor et al., 1982). This work provides a unique approach for validating a simple Gaussian spore transport model to predict spore transport over long distances. This work sets the foundation for using a model to enhance FHB risk assessment tools (De Wolf et al., 2003; Del Ponte et al., 2009; Schaafsma and Hooker, 2007). Although the simple spore transport model we examined performed well in a long term statistical sense, it produced poor predictions of deposition at daily time resolution; this would need to be improved before being incorporated into current FHB risk assessment tools. Farmers use risk assessment tools to guide disease management decisions (e.g. spraying of fungicides) and need accurate and reliable time-resolved predictions daily. This work could be extended to other airborne plant pathogens such as soybean rust and wheat stem rust in the future.

Shape parameters, *b* and *c*, were used to predict the shape of the dispersal kernels and were similar in magnitude for results predicted by the Gaussian transport model, LS transport model, and field observations (Table 3). This result allows us to conclude that a simple Gaussian model was reasonably accurate (in a long term average statistical sense) at predicting long distance transport of spores. As the Gaussian and LS models gave similar results, it would be appropriate to use the simpler and user-friendly Gaussian model for future studies looking at the long distance dispersal of plant pathogens. The Gaussian model can be run readily on any computer, smartphone, or tablet, while computations using the LS model would require hours to perform. For this reason, the Gaussian model is preferred for use by farmers and growers anywhere for quick disease predictions.

The dispersal kernel provides the probability density function describing the average spatial distribution of spores from an inoculated field, and this is an important input for regional and national scale epidemiological models to forecast future disease spread. However, it has been shown that small changes in the 'fat tails' of the dispersal kernel, which are caused by small changes in the *b* exponent, can cause order-of-magnitude changes in predicted spread rates (Higgins et al., 2003; Lewis, 1997), since rare, very long distance (>1 km) dispersal events described by the tails of the kernel end up being the dominant factor in predicting the rate of spread.

In both 2011 and 2012, the shape of the dispersal kernel was strongly governed by a power law (dominant *b* parameter) for both the field results and model predictions. When the shape of the disease kernel is governed by a power law, it indicates that atmospheric turbulence is the dominant factor as shown in Eq. (6c) (Aylor, 1999). When spore dispersal is dictated by a power law, spores may be transported much greater distances than those whose dispersal is dictated by an exponential component. The reason for this phenomenon is that a power law results in a 'fat-tail' in the dispersal kernel which does not approach zero as quickly as an exponential law. Dispersal kernels that follow an exponential shape converge to zero with distance more rapidly, as spores do not survive transport due to solar radiation and are thus not viable, or the entire spore column can be washed out either from a major rainfall event or passive deposition if transport is being studied on a large enough scale as shown in Eq. (6d) (Aylor, 1986, 1999; Rotem et al., 1985). It is possible, that our study was not conducted on a large enough scale for solar radiation and deposition to be a factor in transport, due to the short transport times. In 2011, the dispersal kernel and distance of spore transport was slightly over-predicted by the model when compared to results observed in the field (i.e. observed results had a smaller *b* coefficient); however in 2012 the dispersal kernel and distance of spore transport was slightly under-predicted by the model when compared to results observed in the field (i.e. observed results had a larger *b* coefficient); however the magnitude of differences in both years was small.

In order to estimate the total number of spores deposited at any given location away from a source of inoculum, one needs to know the potential source strength, Q_{pot}, and more importantly, the time dependent release rate, $q_0(t)$. Experimentally, prior to the sampling period, we were able to estimate the Q_{pot} as 3.7 billion ascospores from our inoculated fields in both 2011 and 2012 (Prussin II et al., 2014b). Additionally, we had spore release data during the sampling periods indicating the relative number of spores being released from the center of the plot on hourly intervals. This information was used to develop two different estimates for $q_0(t)$. The first estimate was time varying $q_0{}^{tv}(t)$, in which $q_0(t)$ was varied for each time point based on individual hourly spore release data. The second estimate was the identical daily pattern $q_0{}^{idp}(t)$, in which $q_0(t)$ was assumed to be the same for each hour interval of each day based on the average daily spore release patterns. The results comparing the number of spores deposited at various locations predicted by the model to those observed in the field indicated a strong over-prediction by the model in 2011 assuming identical daily pattern $q_0{}^{idp}(t)$ (over-predicted approximately 150 times), and in 2012 assuming either identical daily pattern $q_0{}^{idp}(t)$ or time varying $q_0{}^{tv}(t)$ (over-predicted approximately 630 and 2000 times, respectively). However, in 2011 when time varying $q_0{}^{tv}(t)$ was used, the model only slightly over-predicted spore deposition (over-predicted approximately 3 times). These results indicated that using time-varying $q_0{}^{tv}(t)$ is the best estimate. Furthermore, using a corrected estimate of the number of spores released, obtained after the fact, improves the performance of the time-varying model, indicating that the Gaussian model provides a good long-term statistical average model when the total number of spores released is known. One possible explanation for the failure of *a priori* predictions to agree with field observations is that spore release from a field may be patchy (heterogeneous) in time with a few 'major' release events (Fernando et al., 2000; Paulitz, 1996). This could partially be due to *F. graminearum* perithecia formation and spore release occurring in 'waves' as field conditions become favorable. The time varying $q_0{}^{tv}(t)$ takes into account these 'major' release events, while the identical daily pattern $q_0{}^{idp}(t)$ assumes that an identical number of spores are being released every single day under the same average daily pattern. Transport models in the future should prioritize time varying $q_0{}^{tv}(t)$ when attempting to predict spore transport and deposition since it captures the intermittent nature of the release pattern.

Temporal patterns of spore release and spore deposition in the field were not correlated (correlation coefficient of $r = -0.12$ for 2011 and $r = 0.45$ for 2012) (Figs. 5 and 6). It is important to address that spore release data were collected by placing a single volumetric spore sampler (approximately 0.5 m high) in the center of the inoculated field, thus we were only able to monitor spore release for one location in the field. It is possible that spore release is heterogeneous across a field, and consequently there were different release patterns across the fields that were not observed due to varying environmental conditions and the formation of microclimates

across the wheat field (Cutforth and McConkey, 1997; Fernando et al., 2000; Paulitz, 1996). This is one possibility for the disagreement between the deposition results observed in the field and spore release patterns. To validate the ability of an LS model to predict the transport of sporangia (spores) of *Phytopthora infestans*, Aylor et al. (2011) used a network of multiple Rotorod towers located 1 m, 1.5 m, and 3 m directly above inoculated potato fields to quantify the number of sporangia being released. Future work examining *F. graminearum* spore release patterns from a wheat field might include a network of volumetric spore samplers placed across a field to determine if spatial heterogeneity exists.

The greatest unknown input of the current spore transport model continues to be Q and $q_0(t)$ consistent with earlier findings (Aylor, 1986). The release rate $q_0(t)$ effects both the spatiotemporal distribution of spore deposition as well as its average (reflected in the dispersal kernel). Thus, we would expect improved accuracy with better a priori estimates of Q and q_0. Prussin II et al. (2014b) estimated Q, and found differences between laboratory estimates and field estimates, which would impact model predictions. Thus, when estimating Q and q_0 it is important to do so under field conditions.

Using our field results, we were able to estimate the overall dispersal kernel for the entire sampling period, and from this, generate an a posteriori estimate for the source strength Q of approximately 3.2 billion spores and 2.1 million spores for 2011 and 2012, respectively, which is approximately 86 and 0.06% of the potential source strength Q_{pot}, respectively. This difference is consistent with earlier estimates suggesting uncertainty in the actual source strength is around three orders of magnitude (Aylor, 1986). Previous research has suggested that both *F. graminearum* perithecia formation and spore release are highly dependent on environmental conditions (Dufault et al., 2006; Fernando et al., 2000; Trail et al., 2002; Tschanz et al., 1975; Xu, 2003). The 2012 field campaign was started approximately a month earlier than in 2011 due to a mild winter and earlier growth of the wheat crop. In 2012, it is possible that environmental conditions were not as conducive for spore release from perithecia as in 2011. This speculation could be assessed with future studies capturing spores with the volumetric spore sampler for a longer time period (e.g., before and after the ~2 week time window considered here) to see if delays occur in spore release or if the potential source is significantly different between seasons, even when the same amount of inoculum is released. Additional studies should also address the effect of a complex of different environmental factors on spore release from perithecia.

Fusarium graminearum spores are first released from perithecia on debris of corn and small grains lying on the ground; however the height of the wheat canopy is approximately 1 m. In order for spores to be released from the crop canopy, they must go from the laminar boundary layer to the turbulent layer and this vertical flux of spores is known to be significantly correlated with atmospheric turbulence (Aylor and Flesch, 2001). Many environmental factors affect turbulence in a wheat field (Lawson and Uk, 1979; Raupach and Thom, 1981). The percentage of spores that escape a crop canopy can be calculated as a function of the height at which spores are released inside the canopy, the settling velocity v_s and the friction velocity u_* (Aylor, 1999; Aylor and Flesch, 2001). The percentage of spores that escape the crop canopy and can be transported long distances increases with an increasing u_*. Aylor and Flesch (2001) computed u_* using wind velocities from a 3D sonic anemometer to obtain horizontal wind profiles, when studying the release of fungal spores from a grass canopy. Unfortunately, we did not use a 3D sonic anemometer in our studies. However, using the log wind profile relationship, we were able to estimate u_* and from that estimate the percentage of spores released that escaped the crop canopy in both 2011 and 2012 (Oke, 1987). We estimated v_s/u_* to be 0.006 and 0.007 for 2011 and 2012, respectively. This implied that approximately 50% of spores that were released escaped the crop canopy in both 2011 and 2012 (Aylor, 1999). Since the estimate of the fraction of spores that escaped the crop canopy in 2011 and 2012 were similar and of order unity, more emphasis should be placed on environmental factors that influence the number of spores being released rather than differences in turbulence between the two field seasons.

The model we examined herein is a simplified model of a real-world scenario. Many assumptions and simplifications were made which might affect the performance of the model, causing it to be accurate in a long term statistical sense but not at a daily time resolution. It is possible that other factors that control spore diffusion and transport in the field experiments might not be properly represented in the model (Gifford, 1982). For example, our model assumes a point source, but our source is actually spatially distributed across a 3716 m^2 plot. However, for large enough distances from the plot center, plots can be approximated as a point source. Also, it is possible that the actual deposition velocity will differ from that shown in Eq. (5a) as we do not take into account wet deposition involving splash loss on the Petri dishes and aerodynamic effects for spores which have a low Stokes number. Additionally, for simplicity in our model, we assume that every ascospore that intercepted the Petri dish became deposited and produced a colony-forming unit; however, it is important to note this assumption would not affect the normalized dispersal kernels because the fraction of spores that intercept a Petri dish and form a colony should be the same at all sampling locations. It is possible that adding more factors to the current spore transport models will improve their predictive ability at daily time resolution (Aylor, 1986, 1999; Aylor et al., 1982, 2011).

The simple long distance spore transport model we examined was able to correctly predict the power law characteristics of spore transport dispersal kernels when compared to results observed in two independent field studies, indicating an appropriate model to predict spore transport from a known source of inoculum. Given the limitations in our ability to provide an accurate time-resolved release rate q_0(t) as an input, our model provides some statistical agreement, while not providing time-resolved agreement. Future work should examine how to improve the estimate for $q_0(t)$. Additionally, an increased understanding of all the environmental factors that trigger spore release of *F. graminearum* is needed. This work provides a foundation for the future improvement of spore transport models that may enhance the utility of risk assessment models for plant disease.

Acknowledgments

This material is based upon work supported by the National Science Foundation under Grant Numbers DEB-0919088 (Atmospheric transport barriers and the biological invasion of toxigenic fungi in the genus *Fusarium*), CMMI-1100263 (Dynamical mechanisms influencing the population structure of airborne pathogens: Theory and observations), DGE-0966125 (IGERT: MultiScale Transport in Environmental and Physiological Systems (MultiSTEPS)), AGS-1255662 (CAREER: A Multiscale Study of Heavy Particle Transport in Sparse Canopies), IDR CBET-PDM 113458 (IDR-Collaborative Research: The Impact of Green Infrastructure on Urban Microclimate and Energy Use), and Virginia Small Grains Board proposal numbers 11-2660-06 and 12-2562-05 (Tracking the long-distance transport of the fungus that causes Fusarium head blight in wheat and barley). The authors would also like to acknowledge Dr. Eric Pardyjak for his advice and technical support on the implementation of the QUIC modeling system. Any opinions, findings, and

conclusions or recommendations expressed in this material are those of the authors and do not necessarily reflect the views of the National Science Foundation or the Virginia Small Grains Board.

Appendix A.

The Lagrangian dispersion modeling system used in this study was originally developed to model particle transport around buildings in the urban canopy layer. It consists of two main components: a wind model and a dispersion model. The basic equations for both the wind and plume models are based on the Quick Urban and Industrial Complex (QUIC) dispersion modeling system (Gowardhan et al., 2008; Pardyjak and Brown, 2001; Singh et al., 2008a,b; Brown et al., 2013). The wind model, QUIC-URB rapidly simulates time-averaged three-dimensional winds within complex arrangements of buildings using a mass consistent diagnostic wind model based on Röckle (1990). In this approach, an initial wind field is prescribed based on an upwind boundary-layer profile (e.g., power-law, log-law, urban canopy, or user-specified profile), an incident flow angle, and building geometry. For vegetated regions, QUIC-URB includes parameterization for continuous canopies (Pardyjak et al., 2008) and windbreaks and rows of vegetation (Speckart and Pardyjak, 2014). Once the flow field modifications have been made, the flow field is forced to be mass consistent with the weak constraint that the differences between the initial and final velocity fields be minimized (e.g. Kaplan and Dinar, 1996).

The dispersion model, QUIC-PLUME, is an unsteady "urbanized" random-walk model that contains a non-local mixing scheme and more drift terms than the traditional random-walk model in order to account for turbulence inhomogeneity (see Williams et al., 2004). The methodology is an application of Langevian equations given by Williams et al. (2002) where the drift and diffusion terms are calculated using the mean velocity field gradients from QUIC-URB. The three-dimensional QUIC-PLUME dispersion model is similar to the two-dimensional LS model of Aylor and Flesch (2001).

Deposition of particles in QUIC-PLUME onto vegetative elements is modeled using an extension of the windbreak deposition model of Raupach et al. (2001) to general plant canopies (Pardyjak et al., 2009). The reduction in particle concentration in a vegetative grid cell in the domain is assumed to be a function of the frontal area density of the vegetation, the distance a particle travels while passing through the vegetation, the particles velocity, and a particle deposition conductance. The deposition conductance includes deposition through inertial impaction and Brownian diffusion (see Raupach et al., 2001 for details).

A.1. Numerical implementation

A single simulation domain was used for the 2011 and 2012 release simulations. The QUIC domain was chosen to encompass the entire experimental area covered by each of the experiments. It covered a horizontal region of 1650 m by 1650 m and a vertical extent of 75 m. The domain was discretized using 100 evenly spaced points in the horizontal and 50 exponentially spaced points in the vertical direction. The lowest vertical point started at 0.2 m above the ground surface with the grid spacing increasing by an exponential growth factor of 0.2 above this point. The entire domain surface was covered with a 1-m high homogeneous wheat canopy with a specified canopy attenuation coefficient of 2.45 (the default QUIC-URB value for a wheat canopy). During each 15-min period, the initial velocity profile required by QUIC-URB was specified everywhere using the stability corrected log-law with 2-m wind speed and direction and atmospheric stability taken from a nearby weather station. Atmospheric stability was estimated based on the Pasquill stability class.

The spore source was modeled as a 60 m by 60 m homogeneous area source placed at the top of the canopy (at a height of 1 m). Test simulations using a ground based or volumetric source showed similar dispersion trends to a canopy top area source. For each 15 min period, particles where released from random locations in the source area. The number of particles released n for each time period was chosen based on a target spore concentration quantification level c_T such that $n = M/(c_T\, dxdydz)$ where M is the total spore mass released during a specified time period and dx, dy, and dz are the average grid spacing in the streamwise, spanwise, and vertical directions, respectively. The target spore concentration quantification level c_T is the minimum average concentration that can be resolved if one particle is in the averaging volume during a time step (i.e., $c_T = 1/\Delta t \int C_{\min} dt$, where $C_{\min}$ = mass/volume for one particle). Two target particle concentration quantification levels where tested, $c_T = 10^{-9}$ and $c_T = 10^{-10}$. This resulted in approximately 2×10^6 and 2×10^8 particles released per simulation, respectively. Results presented in section 3 were only minimally impacted by the chosen c_T value and therefore, only results with $c_T = 10^{-10}$ are presented. Particle characteristics (size, density, settling velocity) where chosen to match those used in the Gaussian plume model. Four simulations with QUIC where performed with spore release rates corresponding to the 2011 and 2012 $q_0{}^{tv}(t)$ and $q_0{}^{idp}(t)$ cases.

Appendix B. Supplementary data

Supplementary data associated with this article can be found, in the online version, at http://dx.doi.org/10.1016/j.agrformet.2014.12.009.

References

Aylor, D.E., 1986. A framework for examining inter-regional aerial transport of fungal spores. Agric. For. Meteorol. 38 (4), 263–288.
Aylor, D.E., 1999. Biophysical scaling and the passive dispersal of fungus spores: relationship to integrated pest management strategies. Agric. For. Meteorol. 97 (4), 275–292.
Aylor, D.E., Flesch, T.K., 2001. Estimating spore release rates using a Lagrangian stochastic simulation model. J. Clim. Appl. Meteorol. 40 (7), 1196–1208.
Aylor, D.E., Sanogo, S., 1997. Germinability of Venturia inaequalis conidia exposed to sunlight. Phytopathology 87 (6), 628–633.
Aylor, D.E., Sutton, T.B., 1992. Release of *Venturia inaequalis* ascospores during unsteady rain: relationship to spore transport and deposition. Phytopathology 82 (5), 532–540.
Aylor, D.E., Taylor, G.S., Raynor, G.S., 1982. Long-range transport of tobacco blue mold spores. Agric. Meteorol. 27 (3–4), 217–232.
Aylor, D.E., Schmale III, D.G., Shields, E.J., Newcomb, M., Nappo, C.J., 2011. Tracking the potato late blight pathogen in the atmosphere using unmanned aerial vehicles and Lagrangian modeling. Agric. For. Meteorol. 151 (2), 251–260.
Bai, G., Shaner, G., 2004. Management and resistance in wheat and barley to Fusarium head blight. Annu. Rev. Phytopathol. 42, 135–161.
Brown, M., Gowardhan, A., Nelson, M., Pardyjak, E., 2013. QUIC transport and dispersion modeling of two releases from the Joint Urban 2003 field experiments. Int. J. Environ. Pollut. 52 (3–4), 263–287.
Cutforth, H., McConkey, B., 1997. Stubble height effects on microclimate, yield and water use efficiency of spring wheat grown in a semiarid climate on the Canadian prairies. Can. J. Plant Sci. 77 (3), 359–366.
De Wolf, E.D., Madden, L.V., Lipps, P.E., 2003. Risk assessment models for wheat Fusarium head blight epidemics based on within-season weather data. Phytopathology 93 (4), 428–435.
Del Ponte, E.M., Fernandes, J.M.C., Pavan, W., Baethgen, W.E., 2009. A model-based assessment of the impacts of climate variability on Fusarium head blight seasonal risk in southern Brazil. J. Phytopathol. 157 (11–12), 675–681.
Dill-Macky, R., Jones, R., 2000. The effect of previous crop residues and tillage on Fusarium head blight of wheat. Plant Dis. 84 (1), 71–76.
Dufault, N., De Wolf, E., Lipps, P., Madden, L., 2006. Role of temperature and moisture in the production and maturation of *Gibberella zeae* perithecia. Plant Dis. 90 (5), 637–644.
Fernando, W.G., Miller, J.D., Seaman, W.L., Seifert, K., Paulitz, T.C., 2000. Daily and seasonal dynamics of airborne spores of *Fusarium graminearum* and other Fusarium species sampled over wheat plots. Can. J. Bot. 78 (4), 497–505.
Gifford Jr., F.A., 1961. Use of routine meteorological observations for estimating atmospheric dispersion. Nucl. Saf. 2, 47–51.
Gifford Jr., F.A., 1968. An Outline of Theories of Diffusion in the Lower Layers of the Atmosphere. Environmental Science Services Administration, Oak Ridge, TN.

Gifford, F., 1982. Horizontal diffusion in the atmosphere: a Lagrangian-dynamical theory. Atmos. Environ. (1967) 16 (3), 505–512.
Gowardhan, A.A., Brown, M.J., Pardyjak, E.R., 2008. Evaluation of a fast response pressure solver for flow around and isolated cube. J. Wind Eng. Ind. Aerodyn. 10, 211–328.
Gregory, P.H., 1961. The Microbiology of the Atmosphere. Leonard Hill, London.
Higgins, S., Nathan, R., Cain, M., 2003. Are long-distance dispersal events in plants usually caused by nonstandard means of dispersal? Ecology 84 (8), 1945–1956.
Irwin, J.S., Petersen, W.B., Howard, S.C., 2007. Probabilistic characterization of atmospheric transport and diffusion. J. Appl. Meteorol. Climatol. 46 (7), 980–993.
Isard, S.A., Gage, S.H., Comtois, P., Russo, J.M., 2005. Principles of the atmospheric pathway for invasive species applied to soybean rust. Bioscience 55 (10), 851–861.
Kaplan, H., Dinar, N., 1996. A lagrangian fispersion model for calculating concentration distribution within a built-up domain. Atmos. Environ. 30 (24), 4197–4207.
Keller, M.D., Waxman, K.D., Bergstrom, G.C., Schmale III, D.G., 2010. Local distance of wheat spike infection by released clones of *Gibberella zeae* disseminated from infested corn residue. Plant Dis. 94 (9), 1151–1155.
Keller, M.D., Thomason, W.E., Schmale III, D.G., 2011. The spread of a released clone of *Gibberella zeae* from different amounts of infested corn residue. Plant Dis. 95 (11), 1458–1464.
Krupa, S., et al., 2006. Introduction of Asian soybean rust urediniospores into the midwestern United States – a case study. Plant Dis. 90 (9), 1254–1259.
Lawson, T., Uk, S., 1979. The influence of wind turbulence, crop characteristics and flying height on the dispersal of aerial sprays. Atmos. Environ. (1967) 13 (5), 711–715.
Lewis, M.A., 1997. Variability, patchiness, and jump dispersal in the spread of an invading population. In: Spatial Ecology: The Role of Space in Population Dynamics and Interspecific Interactions. Princeton University Press, Princeton, New Jersey, United States, pp. 46–69.
Livingston, M., et al., 2004. Economic and Policy Implications of Wind-Borne Entry of Asian Soybean Rust into the United States. US Department of Agriculture, Economic Research Service.
Maldonado-Ramirez, S.L., Schmale III, D.G., Shields, E.J., Bergstrom, G.C., 2005. The relative abundance of viable spores of *Gibberella zeae* in the planetary boundary layer suggests the role of long-distance transport in regional epidemics of Fusarium head blight. Agric. For. Meteorol. 132 (1–2), 20–27.
McMullen, M., Jones, R., Gallenberg, D., 1997. Scab of wheat and barley: a re-emerging disease of devastating impact. Plant Dis. 81 (12), 1340–1348.
Nita, M., De Wolf, E., Isard, S., 2008. Decline in Viability of *Gibberella zeae* Ascospores After Exposure to the Solar Radiation. National Fusarium Head Blight Fourm, Indianapolis, IN.
Oboukhov, A., 1962. Some specific features of atmospheric turbulence. J. Fluid Mech. 13 (1), 77–81.
Oke, T.R., 1987. Boundary Layer Climates, 2nd ed. Cambridge University Press, Cambridge, UK.
Pan, Z., et al., 2006. Long-term prediction of soybean rust entry into the continental United States. Plant Dis. 90 (7), 840–846.
Pardyjak, E.R., Brown, M.J., 2001. Evaluation of a fast-response urban wind model-comparison to single-building wind-tunnel data. In: Proceeding of the 2001 International Symposium on Environmental Hydraulics, Tempe, AZ.
Pardyjak, E.R., Speckart, S., Yin, F., Veranth, J.M., 2008. Near-source deposition of vehicle-generated fugitive dust on vegetation and buildings: model development and theory. Atmos. Environ. 42, 6442–6452.
Pardyjak, E.R., Amatul, U.N., Nelson, M.A., Brown, M.J., 2009. Development of a vegetation deposition model for a fast response urban Lagrangian dispersion model. In: American Meteorological Society, Eighth Symposium on the Urban Environment, Phoenix, AZ, 10–16 January 2009.
Pasquill, F., 1976. Atmospheric Dispersion Parameters in Gaussian Plume Modeling. Part 2: Possible Requirements for Change in the Turner Workbook Values. Environmental Protection Agency, EPA Publication No. EPA-600/4-76-030b. Office of Air Quality Planning & Standards, North Carolina, United States.
Pasquill, F., Michael, P., 1977. Atmospheric diffusion. Phys. Today 30, 55.
Paulitz, T.C., 1996. Diurnal release of ascospores by *Gibberella zeae* in inoculated wheat plots. Plant Dis. 80 (6), 674–678.
Paulitz, T.C., 1999. Fusarium head blight: a re-emerging disease. Phytoprotection (Québec) 80 (2), 127–133.
Prussin II, A.J., Li, Q., Malla, R., Ross, S.D., Schmale III, D.G., 2014a. Monitoring the long distance transport of *Fusarium graminearum* from field-scale sources of inoculum. Plant Dis. 98 (4), 504–511.
Prussin II, A.J., Szanyi, N.A., Welling, P.I., Ross, S.D., Schmale III, D.G., 2014b. Estimating potential source strength of a field-scale source of *Fusarium graminearum* inoculum. Plant Dis. 98 (4), 497–503.
Raupach, M., Thom, A., 1981. Turbulence in and above plant canopies. Annu. Rev. Fluid Mech. 13 (1), 97–129.
Raupach, M.R., Woods, N., Dorr, G., Leys, J.F., Cleugh, H.A., 2001. The entrapment of particles by windbreaks. Atmos. Environ. 35, 3373–3383.
Röckle, 1990. Bestimmung der Stomungsverhaltnisse im Bereich komplexer Bebauungsstrukturen. Vom Fachbereich Mechanik, der Technischen Hochschule, Darmstadt, Germany.
Rotem, J., Wooding, B., Aylor, D., 1985. The role of solar radiation, especially ultraviolet, in the mortality of fungal spores. Phytopathology 75 (5), 510.
Schaafsma, A., Hooker, D., 2007. Climatic models to predict occurrence of *Fusarium* toxins in wheat and maize. Int. J. Food Microbiol. 119 (1), 116–125.
Schmale III, D.G., Bergstrom, G.C., 2003. Fusarium head blight in wheat. Plant Health Instr. Online Publication. http://dx.doi.org/10.1094/PHI-I-2003-0612-01
Schmale III, D.G., Arntsen, Q.A., Bergstrom, G.C., 2005. The forcible discharge distance of ascospores of *Gibberella zeae*. Can. J. Plant Pathol. 27 (3), 376–382.
Schmale III, D.G., et al., 2006. Genetic structure of atmospheric populations of *Gibberella zeae*. Phytopathology 96 (9), 1021–1026.
Schmale III, D.G., et al., 2012. Isolates of *Fusarium graminearum* collected 40–320 meters above ground level cause Fusarium head blight in wheat and produce trichothecene mycotoxins. Aerobiologia 28 (1), 1–11.
Seinfeld, J.H., Pandis, S.N., 2006. Atmospheric Chemistry and Physics – From Air Pollution to Climate Change, 2nd ed. John Wiley & Sons, New York.
Singh, R.P., et al., 2006. Current status, likely migration and strategies to mitigate the threat to wheat production from race Ug99 (TTKS) of stem rust pathogen. CAB Rev. 054, 1–13, http://dx.doi.org/10.1079/PAVSNNR20061054.
Singh, B., et al., 2008a. Evaluation of the QUIC-URB fast response urban wind model for a cubical building array and wide building street canyon. Environ. Fluid Mech. 8, 281–312.
Singh, R.P., et al., 2008b. Will stem rust destroy the world's wheat crop? Adv. Agron. 98, 271–309.
Snijders, C.H.A., 1990. Fusarium head blight and mycotoxin contamination of wheat: a review. Eur. J. Plant Pathol. 96 (4), 187–198.
Speckart, S., Pardyjak, E., 2014. A method for rapidly computing windbreak flow field variables. J. Wind Eng. Ind. Aerodyn. 132, 101–108.
Stokstad, E., 2007. Deadly wheat fungus threatens world's breadbaskets. Science 315 (5820), 1786–1787.
Sutton, J., 1982. Epidemiology of wheat head blight and maize ear rot caused by *Fusarium graminearum*. Can. J. Plant Path. 4 (2), 195–209.
Trail, F., Xu, H., Loranger, R., Gadoury, D., 2002. Physiological and environmental aspects of ascospore discharge in *Gibberella zeae* (anamorph *Fusarium graminearum*). Mycologia 94 (2), 181–189.
Trail, F., Gaffoor, I., Vogel, S., 2005. Ejection mechanics and trajectory of the ascospores of *Gibberella zeae* (anamorph *Fuarium graminearum*). Fungal Genet. Biol. 42 (6), 528–533.
Tschanz, A., Horst, K., Nelson, P.E., 1975. Ecological aspects of ascospore discharge in *Gibberella zeae*. Phytopathology 65, 597–599.
Turner, D.B., 1970. Workbook of Atmospheric Dispersion Estimates. US Department of Health, Education, and Welfare, National Center for Air Pollution Control.
Vogelgsang, S., Widmer, F., Jenny, E., Enkerli, J., 2009. Characterisation of novel *Fusarium graminearum* microsatellite markers in different *Fusarium* species from various countries. Eur. J. Plant Pathol. 123 (4), 477–482.
Williams, M.D., Brown, M.J., Pardyjak, E.R., 2002. Development and testing of a dispersion model for flow around buildings. In: 4th AMS Symposium on the Urban Environment, American Meteorological Society, Norfolk, VA.
Williams, M.D., et al., 2004. Testing of the QUIC-plume model with wind-tunnel measurements for a high-rise building. In: 5th AMS Symposium on the Urban Environment, American Meteorological Society, Vancouver, BC.
Xu, X., 2003. Effects of environmental conditions on the development of Fusarium ear blight. Eur. J. Plant Pathol. 109 (7), 683–689.